

REACTIVELY SPUTTERED Cu_2S FILMS AND Cu_2S -CdS SOLAR CELLS

Eddy VANHOECKE, Marc BURGELMAN and Lieven ANAF

Chent State University, Belgium
Laboratorium voor Elektronika en Meettechniek
Sint Pietersnieuwstraat 41
B - 9000 GENT , Belgium

ABSTRACT

Copper sulfide films are formed on glass by sputtering a copper target in a $\text{H}_2\text{S}/\text{Ar}$ atmosphere. The properties of the films are investigated by various electrical and optical measurements, while the sputtering parameters are varied. Films with a suited stoichiometry, crystallography and resistivity for solar cell application are then sputtered onto evaporated CdS films. The influence of some parameters such as the CdS thickness, chemical and sputter etching, the Cu_2S thickness and post fabrication annealing on the solar cell characteristics is investigated. The best cell obtained is characterized by : $J_{\text{SC}} = 13.75 \text{ mA/cm}^2$, $V_{\text{OC}} = 0.572 \text{ Volt}$, $\text{FF} = 62,5 \%$, $\eta = 4.9 \%$. A brief discussion is given on these parameters, on J_{SC} versus V_{OC} measurements, on I-V measurements in the dark and on C-V measurements.

INTRODUCTION

The copper sulfide - cadmium sulfide thin film solar cells have been studied since many years, and have reached their actual state-of-the-art some years ago (e.g. (1)). In these cells, the copper sulfide layer is commonly formed into an evaporated CdS layer by the well known "wet dipping process". This process is rather critical, and alternatives have been proposed for large scale solar cell production. The reactive sputtering technique is very promising to that purpose : it is well established as an industrial technique for coating large area substrates, and the fabrication of a solar cell could be organised in an all vacuum process, avoiding all wet steps. It should be noted here that even the "dry method" involves a wet step, in which the reaction product CdCl_2 between CdS and an evaporated CuCl layer is washed away. Cu_2S films can be sputtered on any surface; when the films are deposited on glass, electrical and optical measurements are not disturbed by an underlying layer, and are thus more easy to interpret. In the literature reports are given where Cu_2S is sputtered for solar cell application onto single crystal CdS (2), onto evaporated CdS layers (3-9), onto sputtered CdS layers (8, 10-11), and onto evaporated (CdZn)S layers (7,8).

We formed copper sulfide layers by sputtering a pure copper target in an $\text{H}_2\text{S}/\text{Ar}$ gas mixture. The fabrication procedure will be described here, as well as its consequences to the stoichiometric,

crystallographical, optical and electrical properties of the Cu_2S films deposited on glass. We also sputtered Cu_2S layers onto evaporated CdS layers. We will present here the influence of the Cu_2S deposition parameters on the solar cell properties.

Cu_2S DEPOSITION TECHNIQUE

We deposited Cu_2S layers in an R.F. sputtering unit. The target was a 99.998 % pure copper disc with a diameter of 10 cm. The Corning 7059 borosilicate glass substrates were placed 5.5 cm above the target on a water cooled substrate holder. Four substrates of 2.5 cm x 2.5 cm area were coated at a time : two glass substrates previously coated with silver and cadmium sulfide for fabricating solar cells, and two bare glass substrates for characterizing the Cu_2S layer itself. H_2S and Ar gas were premixed in a gas flow system, in such a way that the H_2S -to-argon flow ratio α was regulated automatically to a preset value. The flow ratio α is simply related to the pressure ratio $\text{ppH}_2\text{S}/\text{p}_t$, where ppH_2S is the partial pressure of H_2S , and p_t is the total pressure. As pointed out earlier (9), with the known pumping speeds of our system, α and $\text{ppH}_2\text{S}/\text{p}_t$ have about the same numerical value for the H_2S injection rates of interest. In our apparatus, the R.F. power could also be applied to the substrates, so that the substrates could be sputter cleaned prior to the Cu_2S deposition.

Cu_2S FILMS ON GLASS

Our Cu_2S films sputtered on glass were investigated with X-ray diffraction, by analysing the optical reflection and transmission spectrum $R(\lambda)$ and $T(\lambda)$, and by measuring the resistivity and the Hall mobility. X-ray diffraction allows the identification of the various copper-sulfur phases present in the film; when the film consists of pure copper and pure chalcocite (Cu_2S), the stoichiometry index x of the resulting Cu_xS film can be determined quantitatively (9). When the film contained also copper deficient phases such as djurleite ($\text{Cu}_{1.93}\text{S}$), digenite ($\text{Cu}_{1.8}\text{S}$) or anilite ($\text{Cu}_{1.75}\text{S}$), the crystal structure was so bad that no clear X-ray diffraction peaks could be observed.

To interpret the optical reflection and transmission measurements, we calculated the reflection and transmission of mixtures of pure copper-sulfur

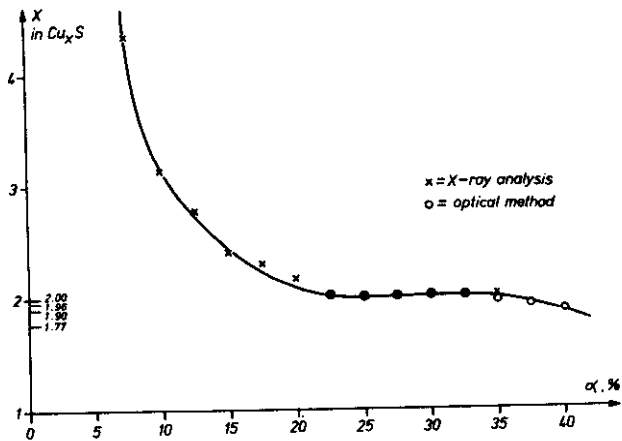


Figure 1 : Stoichiometry index x as a function of the H_2S -to-argon flow ratio α

phases, and fitted them to the measured $R(\lambda)$ and $T(\lambda)$. Doing so, the thickness of the film and its stoichiometry could be determined accurately, when the film consists of chalcocite, or of a mixture of chalcocite and copper-deficient phases, i.e. for $x \leq 2$ (9). These characterization methods lead to the same results as those obtained in the literature, where x was estimated by electron microprobe measurements (2).

The electrical resistivity ρ is closely related to the stoichiometry. The ρ versus x curve has however to be gauged by independent measurements of x , because there is some scattering in the literature data (9). Finally, the form of the $\rho(T)$ curve obtained whilst temperature cycling between room temperature and about $150^\circ C$, is indicative for the mixture of copper-sulfur phases under investigation, and can thus be used for a quick qualitative characterization of the Cu_xS layer. All these characterization methods lead to the following results for Cu_xS films grown on glass (figures 1 and 2) (9) :

For very low H_2S -to-argon flow ratios α , i.e. $\alpha < 5\%$, the deposited films consist of pure copper. For low values of α , i.e. $5\% < \alpha < 22.5\%$, the film consists of a pure chalcocite background,

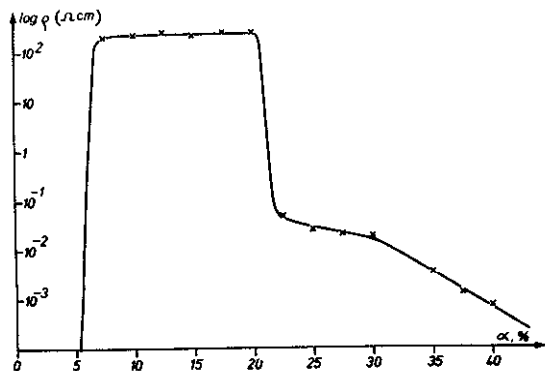


Figure 2 : The electrical resistivity ρ as a function of the H_2S -to-argon flow ratio α .

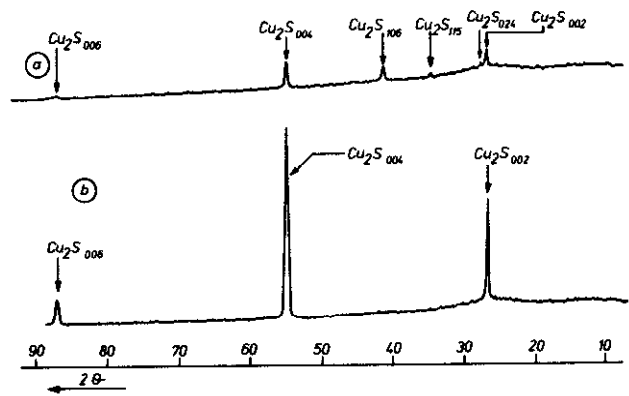


Figure 3 : X-ray diffraction diagram of a Cu_2S film on a glass substrate ; (a) no sputter-etching of the substrate and (b) sputter-etching of the substrate during 10 minutes prior to the Cu_2S deposition.

with isolated copper segregations. The resistivity is high, some $200 \Omega cm$, and is believed to be that of pure and undoped Cu_2S . In an intermediate range, $22.5\% < \alpha < 32.5\%$, the only phase present is chalcocite; it is however not in equilibrium with copper, and therefore not at the copper-rich limit of its existence region, and thus heavily doped (9). This is the α -range suited for solar cell fabrication. For still higher values of α , i.e. $\alpha > 32.5\%$ one obtains mixtures of chalcocite and copper-deficient phases, i.e. $x < 2$.

When the chalcocite is deposited as described it forms very smooth films on glass, the crystallite size being very small ($< 10 nm$). The films grow preferentially with their $(0,0,l)$ plane parallel to the substrate. This can be seen from figure 3a : the intensity ratio of the 004 peak to the 106 peak is 2.35, whereas literature data for powdered Cu_2S give 0.47 (12) or 0.37 (13) for this ratio. The undesired reflection peak of the 106 plane, which makes an angle of 10.8° to the 001 plane, is completely absent when the substrate has been sputter-etched for 10 minutes prior to the Cu_2S deposition (fig. 3b).

The Hall-mobility and the doping concentration were measured on a cross-shaped sample geometry (14). The pure chalcocite films have an acceptor concentration of about $10^{20} cm^{-3}$ and a Hall-mobility of 2 to $4 cm^2/Vs$ (figure 4), whereas the films containing also djurleite show much larger doping concentrations, and a constant mobility. The doping and the mobility of samples containing both copper and chalcocite could not be measured, due to the very high sheet resistance of the film.

Cu_2S FILMS ON CdS

Cu_2S -CdS solar cells were prepared on Corning 7059 substrates of $2.5 cm \times 2.5 cm$ area by successive evaporating a $50 nm$ Cr layer, a $1 \mu m$ Ag layer and a rather thick CdS layer. The substrate temperature for the CdS evaporation was $200^\circ C$ to $210^\circ C$, and the thickness ranged from $5 \mu m$ to $30 \mu m$ (15). Some of these CdS substrates were completed to Cu_2S -CdS solar cells by means of both the "dry

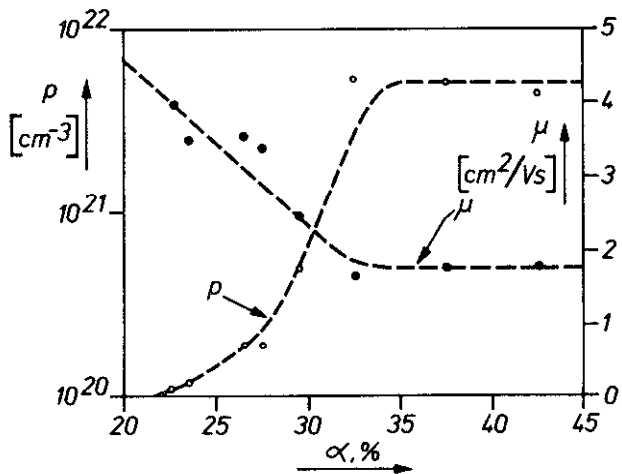


Figure 4 : Hole concentration p and Hall-mobility μ_H as a function of the H_2S -to-argon flow ratio α .

barrier method" (16) and by the conventional wet dipping process, for comparative measurements. The other CdS substrates were loaded in the Cu_2S sputtering apparatus. The H_2S injection rate was such as to obtain pure Cu_2S , without copper segregations; the thickness ranged from 50 nm to 300 nm, and the substrates were not heated.

The Cu_2S geometry was defined by means of a 2 cm x 1.8 cm rectangular molybdenum mask. A 250 nm thick gold grid was evaporated as a front contact; the finger width was 80 μm , and the spacing between the fingers was 700 μm . Finally, a collecting contact was evaporated onto the finger grid; it consists of a 40 nm Au / 1 μm Cu / 40 nm Au sandwich structure, and produces an extra shading of about 6 %, the total grid transmission being thus about 84 %. No anti-reflection coating was applied. Various fabrication parameters were varied to observe their influence on the cell characteristics.

CdS film thickness.

The thickness of the CdS layer is not critical. Good solar cells were obtained for CdS thicknesses ranging from 10 μm to 30 μm . When the CdS film however becomes too thin, e.g. 5 μm , the cells suffer from an excessive shunt conductance and can even be short-circuited. Sputtering of the Cu_2S film can thus lead to a cheaper cell production, when compared to the wet dipped cells, since the CdS thickness for the latter has to be at least 30 μm , and since the CdS film accounts for more than 30 % of the solar cell material cost (17).

Etching: the CdS substrate.

The CdS samples were sputter cleaned prior to the Cu_2S deposition. Typical parameters are : 0.4 Pa pressure, 600 V D.C. voltage during 10 minutes. The resulting substrate etching speed was about 7.5 nm/min. This substrate sputter etching resulted in a better crystallographic orientation of the Cu_2S film : the 106 to 004 peak height ratio

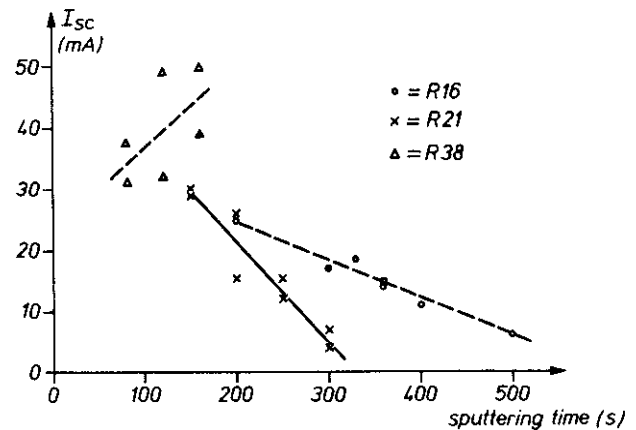


Figure 5 : Short circuit current I_{sc} as a function of the deposition time, for different fabrication runs.

dropped by a factor of about 2; it did however not drop to zero as was the case for Cu_2S films on glass. This is due to the imperfect crystallographical orientation of the thick CdS film (15).

Some of the CdS samples were also chemically etched during 5 s to 40 s in a diluted HCl solution (25 % by volume) at 60 °C. The etch rate is then about 85 nm/s. This etch enhances the CdS surface roughness, resulting in an improvement of about 25 % of the light current due to increased light trapping, to a decrease of about 10 mV of the open circuit voltage, due to an increase of the junction area, and to an extra fill factor loss. As a result the efficiency improved by about 0.35 % (absolutely) by the HCl etch.

Cu₂S film thickness.

During the sputtering of Cu_2S , the R.F. power was adjusted to give a D.C. voltage of 1600 Volt at the target. The H_2S -to-argon flow ratio α was between 25 % and 30 %, and the total pressure was 0.4 Pa. This resulted in the deposition of pure chalcocite at a rate of about 0.6 nm/s. The sputtering time ranged from 80 s to 500 s, the Cu_2S thickness from 50 nm to 300 nm, and the Cu_2S sheet resistance from 250 Ω to 1500 Ω . The thinner films have a better collection efficiency, but they also have a slightly greater sheet resistance and hence a fill factor loss due to a higher series resistance. The best results were obtained for thicknesses ranging from 100 nm to 150 nm (figure 5).

Annealing of the cell.

As deposited cells show no photovoltaic effect and behave as a very small resistance. Annealing in air at an elevated temperature gradually produces the solar cell diode characteristics as shown in figure 6. The optimum air heat treatment seems to be : heating at 160°C during 60 minutes. Annealing in vacuum gives the same results at lower temperatures and for shorter times : 10 to 30 minutes at 140°C is the best vacuum annealing.

R59-7

Consecutive annealing
in air 160°C

- 0- as deposited
- 1- 10 min
- 2- 20 min
- 3- 30 min
- 4- 40 min
- 5- 60 min
- 6- 90 min

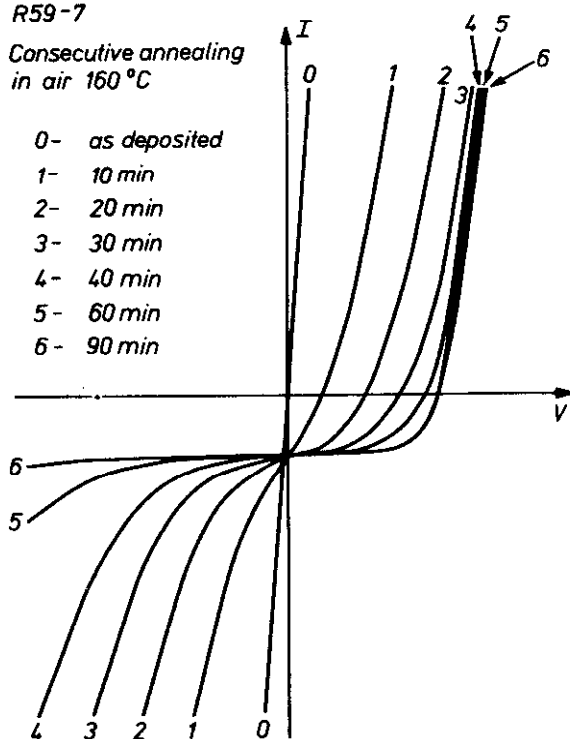


Figure 6 : I-V plot under illumination for a solar cell, when it is annealed six times consecutively in air.

This behaviour of our cells is in contrast with what is reported for other sputtered Cu_2S /evaporated CdS solar cells in the literature, which do show a photovoltaic effect before any annealing (7,8).

Cu_2S -CdS SOLAR CELL CHARACTERIZATION

I-V Characteristics.

The I-V characteristic of the best of our sputtered solar cells is shown in figure 7. The CdS layer was 20 μm thick; there was no HCl etch, but the CdS was sputter-cleaned during 10 minutes. The Cu_2S layer was then sputtered during 200 s with an H_2S -to-argon flow ratio of 25 %. The cell was annealed in air at 160°C during 70 min. There was no anti-reflection coating.

I-V data of some of the better cells are shown in Table I.

TABLE I

Performance of some sputtered Cu_2S /evaporated CdS solar cells.

Cell no.	$J_{sc}(\text{mA}/\text{cm}^2)$	$V_{oc}(\text{mV})$	FF(%)	$\eta(\%)$
R25-6	13.75	572	62.5	4.9
R26-4	11.8	612	58	4.2
R25-2	11.25	565	66	4.2
R38-6	13.8	500	59	4.1
R30-5	13.5	530	57.5	4.1

All the efficiencies were calculated with the total Cu_2S area of 3.6 cm^2 . We will compare our cells

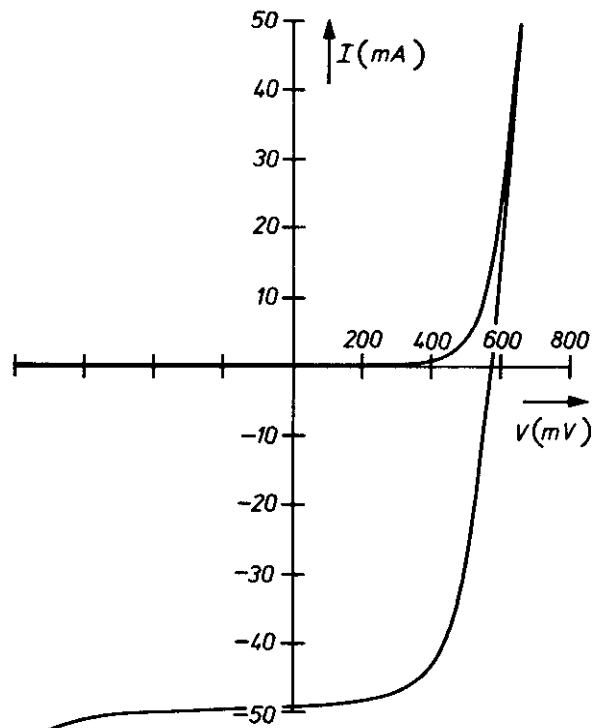


Figure 7 : The I-V plot of the best sputtered Cu_2S -evaporated CdS solar cell. The area is 3.6 cm^2 and the efficiency η is 4.9 % .

with the hybrid sputtered Cu_2S -evaporated CdS solar cell reported in the literature (7,8). No comparison should be made with $\text{Cu}_2\text{S}/(\text{CdZn})\text{S}$ cells, because the latter have an open circuit voltage and thus an efficiency that is intrinsically higher.

The short circuit current of our cells is substantially lower than the best cells in the literature, but the open circuit voltage is substantially higher; this gives a comparable efficiency, because the fill factor is about the same. With open circuit voltages as large as 570 mV, one would expect lossless fill factors that are some 15 % to 20 % (absolutely) higher than the fill factors we actually reach (18). We ascribe this fill factor loss to the large series resistance; it should be avoided by using a contact grid with a smaller finger spacing. One of the main reasons of our too low short circuit current is the bad grid transmission of 84 %, and the absence of any anti-reflection coating.

The open circuit voltage V_{oc} .

All our cells show a high open circuit voltage, which is often more than 550 mV. One cell showed 612 mV, which is the highest open circuit voltage ever reported on a Cu_2S -CdS solar cell. Our V_{oc} measurements were performed under the Standard Test Conditions prescribed by the CEC (19) (This means i.a. measurement under AM1 light, at 25 \pm 2°C). Following Rothwarf and Barnett the open circuit voltage of a Cu_2S -CdS cell is given by (18) :

$$V_{oc} = \frac{\Phi_B}{q} - \frac{AkT}{q} \ln \frac{qN_C S_I}{J_{sc}} - \frac{AkT}{q} \ln \frac{A_j}{A_1} \quad (1)$$

Φ_B is the barrier height and is given by $\Phi_B = E_g - \Delta\chi$ where $E_g \approx 1.2$ eV is the Cu_2S band gap and $\Delta\chi \approx 0.2$ eV is the electron affinity mismatch between Cu_2S and CdS ; A is the diode factor, $N_C \approx 2 \cdot 10^{18} \text{ cm}^{-3}$ is the effective density of states in the CdS conduction band, S_I is the recombination velocity at the interface, A_j is the junction area and A_1 is the normal area of the cell. We assume that our sputtered cells form planar junctions, so that the last term in eq. (1) is negligible. One can obtain the barrier height Φ_B by measuring V_{oc} as a function of the temperature, and then extrapolating to $T = 0$ K. This is done in figure 8; one finds : $\Phi_B = 0.92$ eV, thus somewhat less than the theoretical value of $E_g - \Delta\chi \approx 1.0$ eV.

One can gain more information if one measures V_{oc} and J_{sc} at various light intensities and at various temperatures. At each temperature, a $\log J_{sc}$ versus V_{oc} diagram displays a straight line; from the slope one finds the diode factor A ; the intercept with the $V_{oc} = 0$ axis is then plotted in an Arrhenius plot versus $1/T$; from this plot one can deduce again the barrier height Φ_B and the value of $qN_C S_I$. This is done in figure 9; one finds : the diode factor is about 1, and not dependent on the temperature; the barrier is $\Phi_B = 0.93$ eV, and $S_I = 1.2 \cdot 10^6 \text{ cm/s}$.

Dark current measurements.

The diode current was also measured in the dark. The measurements were treated in the same way as we treated the diode current measurements under illumination (i.e. the $J_{sc} - V_{oc}$ measurements). We found that the dark diode current was described by a temperature dependent diode factor ranging from 2 to 3; the dark current therefore does not behave as an ideal diode, whereas the light diode current does. The bandstructure of the Cu_2S - CdS junction in the dark differs from that under illumination, resulting in a different diode current mechanism. This phenomenon is closely related to the occurrence of a cross-over between

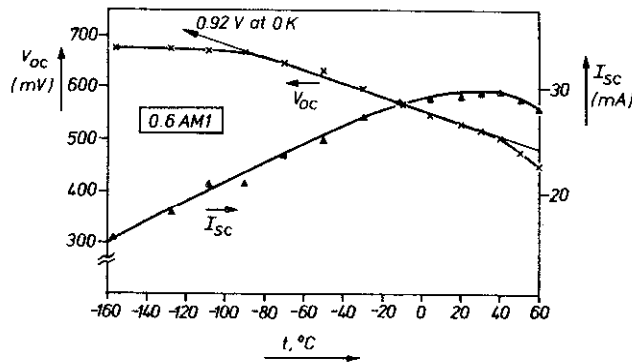


Figure 8 : The temperature dependence of the open circuit voltage V_{oc} and the short circuit current I_{sc} under 0.6 AM1 illumination, of cell R30-5 .

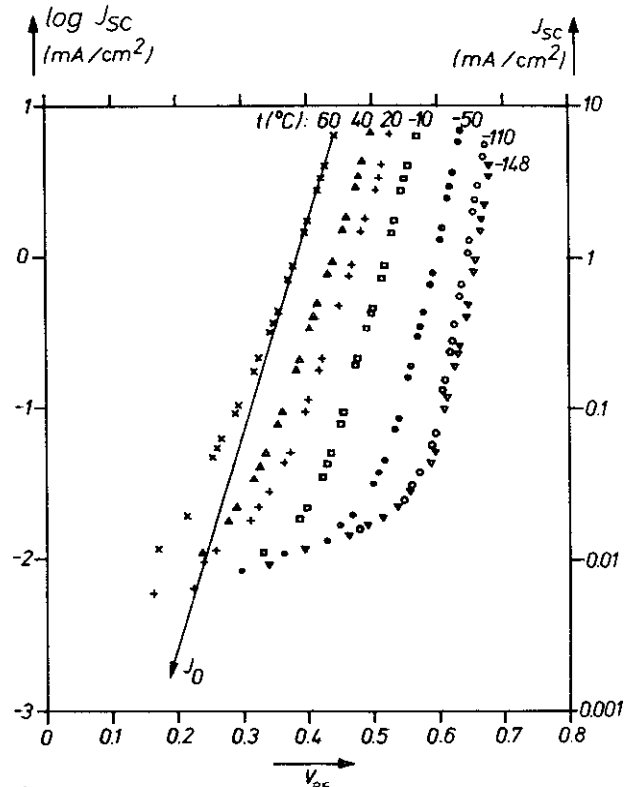


Figure 9a : $\log J_{sc}$ versus V_{oc} for cell R30-5, at various illuminations; the intercept J_0 with the $V_{oc} = 0$ axis is also shown .

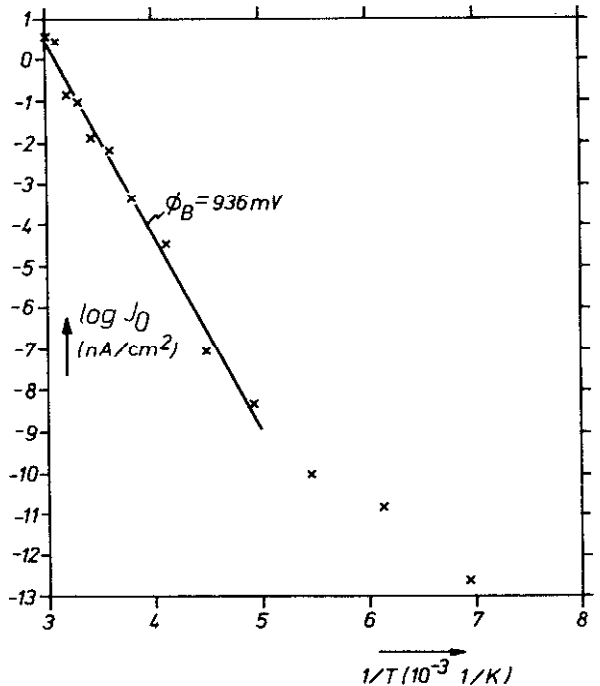


Figure 9b : Arrhenius plot of J_0 from figure 9a : $\log J_0$ versus $1/T$ diagram .

the dark and the light characteristics (20). It should be noted that our best cells show only a very weak cross over; this is due to the relatively low annealing temperatures as compared to some of the dry barrier solar cells (16), which causes only a weak diffusion of Cu atoms from the Cu₂S into the CdS.

Capacitance measurements.

The junction capacity was measured at different frequencies (100 Hz - 100 kHz) and at different reverse voltages (-1.5 V to 0 V), both in the dark and under illumination ($\lambda = 500$ nm, 4 mW/cm²). The capacity versus frequency behaviour was linear, as it is for wet dipped and dry cells; this indicates the existence of a band of deep donor levels in the CdS, as explained in (21). From the capacity versus voltage measurements, we obtained for the best cell (R25-6) : depletion layer width = 0.12 μ m at 0 V, effective donor concentration $\approx 6 \cdot 10^{16}$ cm⁻³. In general the impedance phase angles amounted -85°, proving again the good quality of the sputtered junctions.

ACKNOWLEDGEMENT

This text presents research results of the Belgian National Energy R & D Program (Prime Ministers' Office - Science Policy Programming). The scientific responsibility is assumed by its authors. One of us (M.B.) thanks the National Science Foundation for a fellowship.

REFERENCES

- (1) G. HEWIG et al., Proceedings 16th IEEE Photovoltaic Specialists Conference, San Diego, p. 713-718 (1982).
- (2) G. ARMANTROUT et al., Proceedings 13th IEEE Photovoltaic Specialists Conference, Washington, p. 383-391 (1978).
- (3) L. PARTAIN, G. ARMANTROUT and D. OKUBO, IEEE Trans. Electron Devices, ED-27, 2127-2133 (1980).
- (4) E. ELIZALDE, M. LEON, F. RUEDA and F. ARJONA, Proc. 4th E.C. Photovoltaic Solar Energy Conference, Stresa, p. 809-817 (1982).
- (5) W. ANDERSON, A. JONATH and J. THORNTON, Proc. 2nd E.C. Photovoltaic Solar Energy Conference Berlin, p. 890-897 (1978).
- (6) A. JONATH, W. ANDERSON, J. THORNTON and D. CORNOG, J. Vac. Sci. Technol., 16, 200-202 (1979).
- (7) J. THORNTON, D. CORNOG, R. HALL and L. DiNETTA, J. Vac. Sci. and Technol., 20, 296-299 (1982).
- (8) J. THORNTON et al., Proc. 16th IEEE Photovoltaic Specialists Conference, San Diego, p. 737-742 (1982).
- (9) E. VANHOECKE and M. BURGELMAN, Thin Solid Films, 112, 97-106 (1984).
- (10) W. MULLER, H. FREY, K. RADLER and K.-H. SCHULER, Thin Solid Films, 59, 327-336 (1979).
- (11) J. THORNTON and W. ANDERSON, Applied Physics Letters, 40, 622-624 (1982).
- (12) Powder Diffraction File, Joint Committee on Powder Diffraction Standards, file 23-961.
- (13) R. POTTER and H. EVANS, J. Res. U.S. Geol. Surv., 4, 205-212 (1976).
- (14) G. DE MEY, Advances in Electronics and Electron Physics, 61, 1-61 (1983).
- (15) A. DE VOS, K. STEVENS, L. VANDENDRIESSCHE and M. BURGELMAN, Solar Cells, 8, 33-45 (1983).
- (16) M. BURGELMAN, A. DE VOS and L. VANDENDRIESSCHE Proc. 5th E.C. Photovoltaic Solar Energy Conference, Aθ1VQ1, p. 873-877 (1983).
- (17) W. ARNDT et al., Symposium Micro-79, Banaras Hindu University, Varanasi, India, 15-17 jan. 1979.
- (18) A. ROTHWART and A. BARNETT, IEEE Transactions Electron Devices, 24, 381-387 (1977).
- (19) Standard Procedures For Terrestrial Photovoltaic Performance Measurements, Specification N° 101, Commission of the European Communities (1979).
- (20) P. DE VISSCHERE et al., Proc. 5th E.C. Photovoltaic Solar Energy Conference, Aθ1VQ1, p. 878-882 (1983).
- (21) L. VANDENDRIESSCHE, H. PAUWELS, P. DE VISSCHERE and L. ANAF, to be published in Solid State Electronics (1984).